

APPLICATION OF MODELLING AND SIMULATION TO EVALUATE THE THETA METHOD USED IN DIAGNOSTICS OF AUTOMOTIVE SHOCK ABSORBERS

ZBIGNIEW LOZIA¹

Abstract

The dynamic properties of the car's suspension largely depend on the damping that results from the state of the shock absorbers. Their technical condition is essential for vehicle occupants' comfort and traffic safety. It changes with the time and intensity of use of the vehicle. Therefore, adequate methods of non-destructive (diagnostic) testing of suspension damping have been sought for many years. The on-vehicle tests are particularly useful thanks to their low cost and short test duration time. The newest method is the 'theta' method which is the subject of the presented article. Notation 'theta' usually means relative damping (damping ratio) in the vibrating system. The paper assesses four variants of the method. Two versions come from modal analysis and are also known as the 'peak-picking method' or 'half-power method'. Two other versions are described in cited patent documentations. Three linear 'quarter car' models with their description in the frequency domain were used to assess mentioned variants of the 'theta' method. Calculations were made for two typical datasets corresponding to the front and rear suspension system of a medium-class motor car. This provided grounds for general qualitative and (within a limited scope) quantitative assessment of the usefulness of individual variants of the method under analysis and for comparisons between them. The paper is to help in choosing the variant of the 'theta' method that would most likely find the application and that might be recommended to manufacturers and would-be purchasers of diagnostic suspension testers. The author has also highlighted the importance of possible further research.

Keywords: frequency domain analysis; quarter-car model; theta method; automotive suspension damping; automotive diagnostics

¹ Faculty of Transport, Warsaw University of Technology, Koszykowa 75, 00-662 Warsaw, Poland, e-mail: zbigniew.lozia@pw.edu.pl, ORCID: 0000-0002-3188-545X

1. Introduction

Damping is a very important feature of a mechanical system when one considers its dynamical properties [6, 9, 10]. It changes during the time of system exploitation and intensity of use. There were many attempts to determine (to measure) mechanical system damping [9, 19, 24], including vehicle suspension damping (see works [2-4] or [5, 6, 8] as well as [11-13] or [14, 18, 20], and also [21-23]). It affects the comfort of passengers and traffic safety.

For many years, efforts have been made to develop appropriate methods of testing shock absorbers for diagnostic purposes, especially without disassembly from a vehicle, due to the low cost and short duration of the test. The tests used may be classified in two groups (Figure 1): *'free vibration method'* and *'forced vibration method'* [5, 8]. In the former group, a record of vehicle body vibration (or, more precisely, the number of half-cycles of the vibration) caused by initial test conditions is assessed. In some variants of such an approach, the normal tire-road contact force is measured. This method is not recommended because of its very high sensitivity to the dry friction in the suspension system [25]. In the other group, the vehicle wheel is forced to vibrate vertically with a frequency of (16-25) Hz and then this frequency is gradually reduced until the vibration fades out to 'sweep' the frequency range that covers the natural frequencies of the 'sprung mass' and 'unsprung mass' supported by spring elements of the suspension system and pneumatic tires. In this case, the known fact of high sensitivity of system vibration to damping in the resonance zone is made use of. This group includes the variant proposed by the BOGE company [8, 13, 14], where the initial excitation frequency is about 16 Hz and the peak-to-peak values of vertical displacements of the vibration plate are assessed. Another variant of the *'forced vibration method'* is the one introduced by EUSAMA [e.g. [8, 12, 20] or [21-23]]. In this case, the initial excitation frequency is about 25 Hz and the assessment of the shock absorber condition is based on changes in the force exerted by the tire on the ground [i.e. tester's vibration plate]. An expanded variant of the EUSAMA method is the one proposed by the Hunter company, where the phase shift angle between the excitation (vertical motion of the vibration plate) and the force exerted by the tire on the plate is measured [e.g. [2, 23, 25]].

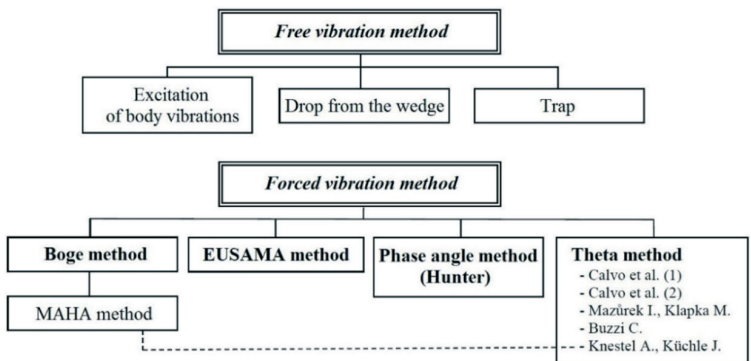


Fig. 1. On-vehicle methods of examining shock absorbers' condition

Recently, increasing importance has been attached to the approach referred to as the 'theta' method, where the relative damping (damping ratio) in the suspension system is assessed (e.g. [3, 4, 5] or [11, 13, 18] as well as [21]). Two versions come from modal analysis and are also known as the 'peak-picking method' or 'half-power method' [9]. The other two versions are described in cited patent documentation [3, 11, 18].

The author has presented a comparative assessment of four 'theta'-type 'forced vibration methods' because more and more manufacturers of diagnostic equipment have recently been attempting to make use of such methods in practice. So, the work presented here is to help in choosing the variant of the 'theta' method that would most likely find application and that might be recommended to manufacturers and would-be purchasers of diagnostic suspension testers.

2. Methodology

The current state of the suspension shock absorber determines suspension relative damping (damping ratio). According to vibration theory (e.g. [7, 9, 10]) it is defined as the ratio of actual viscous damping coefficient value of the suspension system and its critical value (when the free vibration of the system under analysis becomes aperiodic). Frequently used name of this coefficient is 'theta', so the diagnostic method is also called "theta".

The author has used a simulation method based on defined 'quarter car' models. He has chiefly used a model with two degrees of freedom (2DOF), where the impact of the mass of the vibration plate on calculation results is considered. In some variants of the 'theta' method, the model is simplified to one degree of freedom (1DOF). The analysis has been performed in the frequency domain for four variants of the 'theta' method. Calculations have been done for two typical datasets corresponding to the front and rear suspension system of a medium-class motor car.

3. The simulation models used

Below the structures of the models used, equations of motion of a linear 'quarter-car' model with its ancillary parameters as well as model data adopted (corresponding to real vehicle systems) will be discussed.

3.1. Structures of the models used

Among the descriptions of the models of vehicles placed on shock absorber testers, those related to the BOGE method [8, 13, 14] have been left out of account because such a method is no longer used in its original form. Only modification described in [13] to a form close to the 'theta' method has been mentioned. The most complex model of a motor car placed on an on-vehicle shock absorber tester is the one presented in publication [12] – Figure 2. It is

a 3D model with 14 degrees of freedom (DOF), chiefly intended for the simulation of motor vehicle motion on even or rough road surface (including surface with random irregularities). In the application in question, kinematic excitation in a form typical for the EUSAMA method was applied to one (freely chosen) vehicle wheel. The main emphasis was placed on assessment of the impact of damping in the shock absorber that was just not tested and of dry friction in the suspension system, for different states of the shock absorber under test. The calculations were carried out for an independent front suspension system (with couplings through the antiroll bar and vehicle body solid) and a dependent rear suspension system (with couplings through the rear axle solid and vehicle body solid). This model is the best where not only qualitative but also quantitative assessment of test results is essential. On the other hand, the necessity of having a large number of data and characteristics of the complex model is its weak point.

A very popular simplified model is the 'quarter-car' model (see [1, 3, 7] or [10–12] as well as [13–15] or [17, 20, 22], and [23, 25]). It is built by dividing the 3D vehicle model by means of vertical planes into four 'quarter cars'. Apart from the geometrical division, this should be done [1, 10] with simultaneous decomposition of inertial properties, with distinguishing the 'sprung masses', 'unsprung masses', and 'coupling masses' and with applying the mass conservation law and the principle of conservation of moments of inertia and static moments before and after the decomposition. Many authors (e.g. [1, 7, 10] or [11, 12] as well as [15, 17, 22] or [23, 25]) (use a linear form of this model, with a structure as presented in Figure 3a. Some of the authors [17, 22] carry out their analyses with taking also into account the inertia of the vibration plate, which has been shown in Figure 3b.

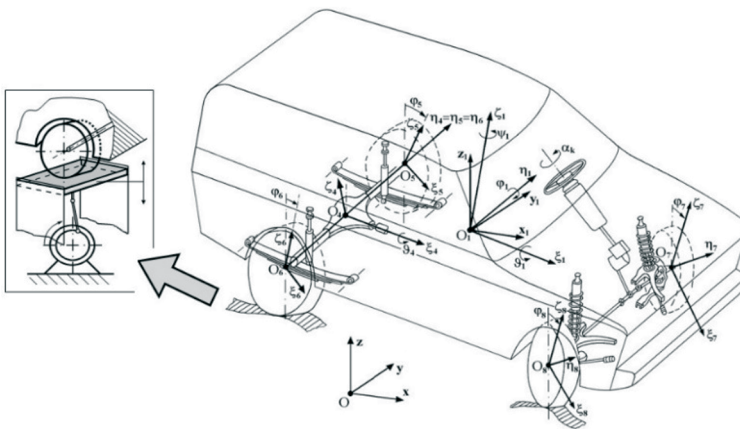


Fig. 2. 3D model of vehicle dynamics with 14 DOF. Kinematic excitation in a form typical for the EUSAMA method applied to freely chosen vehicle wheel [16]

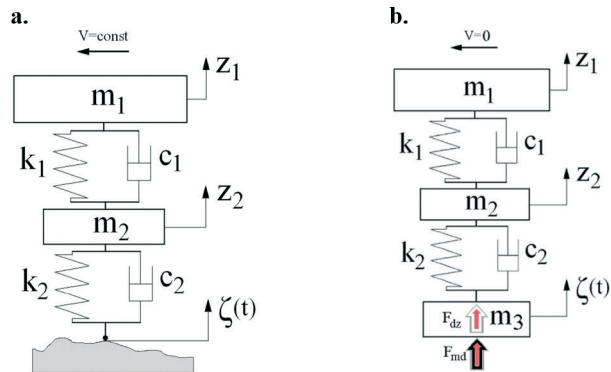


Fig. 3. Linear 'quarter-car' model, where [a] is general version, [b] is version dedicated to the vehicle on a diagnostic tester ($V=0$; the vibration plate inertia is considered)

The authors of publications [11, 25] use a more complex nonlinear 'quarter-car' model, where nonlinearities of suspension and tire elasticity characteristics, 'bouncing' (tire separation from the ground), asymmetry of shock absorber damping curves, and dry friction in the suspension system are considered (in publication [25], five different formal descriptions of dry friction are used).

Other models used in the works cited here have been presented in Figure 4a and b. The one shown in Figure 4a (e.g. [1, 3, 7] or [12]) represents a 1DOF system obtained by disregarding the 'unsprung mass' and adopting an equivalent suspension elasticity (elasticity of the suspension and tire arranged in series). The model represented in Figure 4b is also a 1DOF system intended for the situation where the 'sprung mass' is immobile [13, 18].

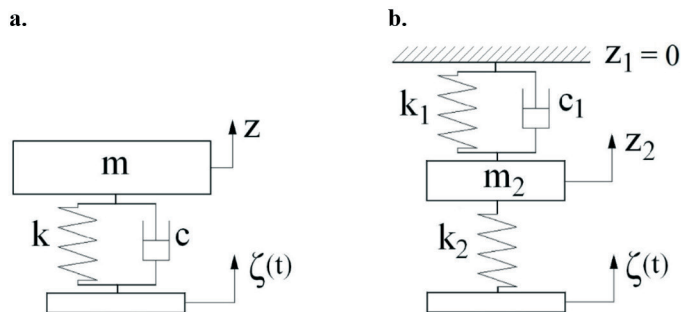


Fig. 4. Simplified 'quarter-car' models, where [a] is 1DOF system obtained by disregarding the 'unsprung mass' and adopting an equivalent suspension elasticity [elasticity of the suspension and tire arranged in series], [b] is another 1DOF system intended for the situation where the 'sprung mass' is immobile

3.2. Equations of motion of a linear 'quarter-car' model with its ancillary parameters

The equations of motion will be presented in a form applicable to the most complex 'quarter-car' model shown in Figure 3b. The other models (Figures 3a, 4a, and b) may be described by simplifying the complex model, which consists of three mass elements, i.e. 'sprung mass' m_1 [kg], 'unsprung mass' m_2 [kg], and vibration plate m_3 [kg]. The suspension and tire stiffness have been denoted by k_1 [N/m] and k_2 [N/m], respectively. Symbols c_1 [N·s/m] and c_2 [N·s/m] represent the viscous damping coefficients of the suspension system and tire, respectively. The kinematic input applied by the vibration plate (exciter) is represented by $\zeta(t)$ [m]. A measuring system measures the input force under the vibration plate. When this force is calculated, other static loads (higher by exciter's plate weight $m_3 \cdot g$, where g is acceleration of gravity) and the force of plate's inertia (with a negative sign) should be considered.

$$N_{st} = (m_1 + m_2) \cdot g \quad (1)$$

$$N_{stm} = (m_1 + m_2 + m_3) \cdot g \quad (2)$$

The tire-exciter contact force F_{op} is a sum of static load N_{st} and dynamic component F_{dz} of the vertical tire force, this component being equal to the sum of dynamic spring force F_{dso} (measured in relation to the state of static equilibrium, i.e. for radial tire deflection in relation to the static deflection) and viscous damping force in the tire F_{two} .

$$F_{op} = F_{dz} + N_{st} \quad (3)$$

$$F_{dz} = F_{dso} + F_{two} \quad (4)$$

The force measured in the diagnostic tester, denoted by F_{opm} , consists of the total tire-exciter contact force F_{op} , which includes other static loads $N_{stm} = (m_1 + m_2 + m_3) \cdot g$, and the force of plate's inertia F_{bp} with a negative sign.

$$F_{opm} = F_{op} - F_{bp} + m_3 \cdot g = F_{op} + m_3 \cdot d^2 \zeta(t) / dt^2 + m_3 \cdot g = F_{dz} + N_{stm} + m_3 \cdot d^2 \zeta(t) / dt^2 = F_{md} + N_{stm} \quad (5)$$

$$F_{bp} = -m_3 \cdot d^2 \zeta(t) / dt^2 \quad (6)$$

$$F_{md} = F_{dz} + m_3 \cdot d^2 \zeta(t) / dt^2 \quad (7)$$

F_{md} is a result of measurement of the dynamic component F_{dz} of the tire force (where the static load N_{st} , N_{stm} is left out). The force of plate's inertia F_{bp} and exciter's plate weight $m_3 \cdot g$ will distort the result of measurement (the value) of force F_{dz} and, in consequence, of force F_{op} . The F_{bp} force also introduces a phase shift of F_{md} in relation to F_{dz} .

In Figure 3b, the dynamic component F_{dz} of the vertical tire-exciter contact force (i.e. the dynamic component of the tire force) has also been shown. This force is applied by tester's vibration plate to the pneumatic tire. The F_{md} force, i.e. the dynamic component of the force

that excites vibration on the tester, measured by tester's measuring system has been shown as well.

The equations of motion in a matrix form have been presented as relation [8]. They have been derived in accordance with the principle of dynamic force analysis, with considering the forces of inertia of individual mass elements of the model. The symbols of the matrices of inertia \mathbf{M} , viscous damping \mathbf{C} , stiffness \mathbf{K} , excitation influences transmitted by damping in the pneumatic tire \mathbf{C}_ζ and excitation influences transmitted by radial stiffness of the pneumatic tire \mathbf{K}_ζ have been highlighted. The vectors of generalized coordinates [displacements], velocities, and accelerations have been denoted by $\mathbf{q}, \dot{\mathbf{q}}, \ddot{\mathbf{q}}$, respectively. This notation has been used in equation [9].

$$\begin{bmatrix} m_1 & 0 \\ 0 & m_1 \end{bmatrix} \cdot \begin{bmatrix} \dot{z}_1 \\ \dot{z}_2 \end{bmatrix} + \begin{bmatrix} c_1 & -c_1 \\ -c_1 & c_1 + c_2 \end{bmatrix} \cdot \begin{bmatrix} z_1 \\ z_2 \end{bmatrix} + \begin{bmatrix} k_1 & -k_1 \\ -k_1 & k_1 + k_2 \end{bmatrix} \cdot \begin{bmatrix} z_1 \\ z_2 \end{bmatrix} = \begin{bmatrix} 0 \\ c_2 \end{bmatrix} \cdot \dot{\zeta} + \begin{bmatrix} 0 \\ k_2 \end{bmatrix} \cdot \zeta \quad (8)$$

$$\mathbf{M} \cdot \ddot{\mathbf{q}} + \mathbf{C} \cdot \dot{\mathbf{q}} + \mathbf{K} \cdot \mathbf{q} = \mathbf{C}_\zeta \cdot \dot{\zeta} + \mathbf{K}_\zeta \cdot \zeta \quad (9)$$

For equation [9], the Laplace transform was formulated, with zero initial conditions. After transformations, equation [10] was obtained, where the domain $s=r+i\omega$ has a real part r and an imaginary part ω and $i^2 = -1$ [ω is the radian frequency [rad/s]]:

$$(\mathbf{M} \cdot s^2 + \mathbf{C} \cdot s + \mathbf{K}) \cdot \mathbf{q}(s) = (\mathbf{C}_\zeta \cdot s + \mathbf{K}_\zeta) \cdot \zeta(s) \quad (10)$$

Its solution has a form [11]

$$\mathbf{q}(s) = (\mathbf{M} \cdot s^2 + \mathbf{C} \cdot s + \mathbf{K})^{-1} \cdot (\mathbf{C}_\zeta \cdot s + \mathbf{K}_\zeta) \cdot \zeta(s) \quad (11)$$

The operational transmittance [transfer function] for displacements [12] is a ratio of the Laplace transform of the output signal to the Laplace transform of the input signal [excitation] of the system at zero initial conditions.

$$\mathbf{H}_q(s) = \begin{bmatrix} H_{q_1}(s) \\ H_{q_2}(s) \end{bmatrix} = \frac{\mathbf{q}(s)}{\zeta(s)} = (\mathbf{M} \cdot s^2 + \mathbf{C} \cdot s + \mathbf{K})^{-1} \cdot (\mathbf{C}_\zeta \cdot s + \mathbf{K}_\zeta) \quad (12)$$

For velocities and accelerations, the operational transmittances are represented by equations [13] and [14], respectively.

$$\mathbf{H}_{\dot{q}}(s) = \begin{bmatrix} H_{\dot{q}_1}(s) \\ H_{\dot{q}_2}(s) \end{bmatrix} = \frac{\dot{\mathbf{q}}(s)}{\zeta(s)} = s \cdot \mathbf{H}_q(s) \quad (13)$$

$$\mathbf{H}_{\ddot{q}}(s) = \begin{bmatrix} H_{\ddot{q}_1}(s) \\ H_{\ddot{q}_2}(s) \end{bmatrix} = \frac{\ddot{\mathbf{q}}(s)}{\zeta(s)} = s^2 \cdot \mathbf{H}_q(s) \quad (14)$$

It is possible to pass from the Laplace transform to the Fourier transform. Thus, the operational transmittances will become spectral transmittances. This may be done by passing from domain s to parameter $i\omega$, with assuming that the real part r in equation $s=r+i\omega$ is equal to zero. The Fourier transform of the dynamic component F_{dz} of the vertical tire-ex-citer contact force is defined by equation [15].

$$F_{dz}(i \cdot \omega) = c_2 \cdot [\dot{\zeta}(i \cdot \omega) - \dot{z}_2(i \cdot \omega)] + k_2 \cdot [\zeta(i \cdot \omega) - z_2(i \cdot \omega)] \quad (15)$$

Based on equations [12]–[15] and in result of appropriate transformations, a compact end form of the spectral transmittance for the dynamic vertical force at the tire–exciter contact point was finally obtained [with remembering that $q_1 = z_1$ and $q_2 = z_2$]:

$$H_{Fdz}(i \cdot \omega) = \frac{F_{dz}(i \cdot \omega)}{\zeta(i \cdot \omega)} = (i \cdot c_2 \cdot \omega + k_2) \cdot [1 - H_{q_2}(i \cdot \omega)] \quad (16)$$

The difference between the dynamic component of the force measured in the tester [F_{md}] and the dynamic vertical force at the tire–exciter contact point [F_{dz}] arises from the force of inertia of tester's vibration plate [exciter].

$$\begin{aligned} H_{Fmd}(i \cdot \omega) &= \frac{F_{md}(i \cdot \omega)}{\zeta(i \cdot \omega)} = \frac{F_{dz}(i \cdot \omega) + m_3 \cdot \ddot{\zeta}(i \cdot \omega)}{\zeta(i \cdot \omega)} = \frac{F_{dz}(i \cdot \omega) - m_3 \cdot \omega^2 \cdot \zeta(i \cdot \omega)}{\zeta(i \cdot \omega)} = \\ &= (i \cdot c_2 \cdot \omega + k_2) \cdot [1 - H_{q_2}(i \cdot \omega)] - m_3 \cdot \omega^2 = H_{Fdz}(i \cdot \omega) - m_3 \cdot \omega^2 \end{aligned} \quad (17)$$

The linear dynamic systems presented [Figures 3a and b, 4a and b] are described by linear systems of ordinary differential equations shown above. Their properties also reflect such quantities [ancillary parameters] as natural radian and Hertz frequencies of undamped systems, critical damping coefficients, and relative damping coefficients.

For the systems of Figures 3a and b, the natural radian frequencies of undamped vibration may be expressed by formula [18] [1, 23].

$$\omega_{01}^2 = \frac{k_1 \cdot m_2 + (k_1 + k_2) \cdot m_1}{2 \cdot m_1 \cdot m_2} \mp \sqrt{\left[\frac{k_1 \cdot m_2 + (k_1 + k_2) \cdot m_1}{2 \cdot m_1 \cdot m_2} \right]^2 - \frac{k_1 \cdot k_2}{m_1 \cdot m_2}} \quad (18)$$

For the system shown in Figure 4a, the value of the natural radian frequency of undamped vibration is defined by formula [19] [e.g. [1, 7, 10]]; for a system of Figure 4b, formula [20] applies [12, 13, 18].

$$\omega_{0a}^2 = \frac{k}{m} \quad (19)$$

$$\omega_{0b}^2 = \frac{k_1 + k_2}{m_2} \quad (20)$$

Between the natural Hertz and radian frequencies of undamped vibration, a general relationship [21] holds [1, 7, 23].

$$f_i = \frac{\omega_i}{2 \cdot \pi} \quad \text{where } i = 01, 02, 0a, 0b \quad (21)$$

The damping is defined as 'critical' when the value of the viscous damping coefficient is such that the free vibration of the system under analysis becomes aperiodic [1, 7, 23].

For the systems of Figures 3a and b, the values of this coefficient are defined by formulas [22] and [23] [23].

$$c_{kr1} = 2 \cdot \sqrt{\frac{k_1 \cdot k_2 \cdot m_1}{k_2 + k_1 \cdot \left(1 + \frac{m_2}{m_1}\right)}} \approx 2 \cdot \sqrt{\frac{k_1 \cdot k_2 \cdot m_1}{k_2 + k_1}} \text{ for } m_1 \gg m_2 \quad (22)$$

$$c_{kr2} = 2 \cdot \sqrt{(k_1 + k_2) \cdot m_2} \quad (23)$$

For the systems shown in Figures 4a and b, these values are defined by formulas [24] [1, 7, 23] and [25] [12, 13, 18], respectively.

$$c_{kra} = 2 \cdot \sqrt{k \cdot m} = 2 \cdot m \cdot \omega_{0a} \quad (24)$$

$$c_{krb} = 2 \cdot \sqrt{(k_1 + k_2) \cdot m_2} = 2 \cdot m_2 \cdot \omega_{0b} = c_{kr2} \quad (25)$$

The relative damping coefficient ϑ_j [-] ['theta'] is calculated as the ratio of the current value of the coefficient of damping in the vehicle suspension system [c or c_I [N·s/m]] to the value of critical damping coefficient c_{Ikrj} [N·s/m], where $j = 1, 2, a, b$. For the systems of Figures 3a and b, the relative damping coefficient values ϑ_1 and ϑ_2 are defined by formulas [26] and [27] [23]; for the systems of Figure 4a, the relative damping coefficient values ϑ_a and ϑ_b are defined by formulas [28] [e.g. [1, 3, 7]] and [29] [12, 18, 23], respectively.

$$\vartheta_1 = c_I / c_{kr1} \quad (26)$$

$$\vartheta_2 = c_I / c_{kr2} \quad (27)$$

$$\vartheta_a = c / c_{kra} \quad (28)$$

$$\vartheta_b = c_I / c_{krb} \quad (29)$$

3.3. Model data adopted, corresponding to real vehicle systems

The calculations were carried out for the 'quarter-car' model data corresponding to the front and rear suspension systems of a medium-class motor car Astra Van. For the front and the rear suspension system, the data were as in Table 1 and in Table 2, respectively.

The parameters describing the simulation test conditions and the adopted values of the relative and absolute damping coefficients ϑ_I and c_I , respectively [corresponding to the models of Figures 3a and b, 4a and b], which most closely represented the structure of the real vehicles under analysis, were as follows: $m_3=14.5$ kg, the lowest Hertz [radian] frequency of the vibration under analysis $f_{min}=0$ [$\omega_{min}=0$], the highest Hertz [radian] frequency of the vibration under analysis $f_{max}=25$ Hz [$\omega_{max}=157.08$ rad/s], the lowest value of the relative coefficient of damping in the suspension system $\vartheta_{Imin}=0.04$, the highest value of the relative coefficient of damping in the suspension system $\vartheta_{Imax}=0.48$, step of changes in the relative coefficient of damping in the suspension system $\Delta\vartheta_I=0.04$, the lowest value of the absolute damping coefficient [corresponding to the lowest relative coefficient of damping in the suspension system ϑ_{Imin}] $c_{Imin}=226.776$ N·s/m [front suspension] and $c_{Imin}=150.796$ N·s/m [rear suspension], the highest value of the absolute damping coefficient [corresponding to the highest relative coefficient of damping in the suspension system ϑ_{Imax}] $c_{Imax}=2\,721.312$ N·s/m

[front suspension] and $c_{1max} = 1\,809.552\text{ N}\cdot\text{s}/\text{m}$ [rear suspension], step of changes in the absolute coefficient of damping [corresponding to the step of changes in the relative coefficient of damping in the suspension system $\Delta\theta_1$] $\Delta c_1 = 226.776\text{ N}\cdot\text{s}/\text{m}$ [front suspension], $\Delta c_1 = 150.796\text{ N}\cdot\text{s}/\text{m}$ [rear suspension].

Table 1. 'Quarter-car' model data [see Figures 3a and b, 4a and b]. The front suspension system of a medium-class motor car Astra Van

Parameter denotation	Value	Unit measure
m	346	kg
m_1	346	kg
m_2	36	kg
k	23 224	N/m
k_1	25 570	N/m
k_2	253 161	N/m
c	variable	N·s/m
c_1	variable	N·s/m
c_2	150	N·s/m
f_{01}	1.30	Hz
f_{02}	14.01	Hz
ω_{01}	8.19	rad/s
ω_{02}	88.03	rad/s
f_{0a}	1.30	Hz
f_{0b}	14.00	Hz
ω_{0a}	8.19	rad/s
ω_{0b}	87.99	rad/s
c_{kr1}	5 669.4	N·s/m
c_{kr2}	6 335.4	N·s/m
c_{kra}	5 669.4	N·s/m
c_{krb}	6 335.4	N·s/m

Table 2. 'Quarter-car' model data [see Figures 3a and b, 4a and b]. The rear suspension system of a medium-class motor car Astra Van

Parameter denotation	Value	Unit measure
m	160	kg
m_1	160	kg
m_2	35	kg
k	22 207	N/m
k_1	24 882	N/m
k_2	206 526	N/m
c	variable	N·s/m
c_1	variable	N·s/m
c_2	150	N·s/m
f_{01}	1.87	Hz
f_{02}	12.96	Hz
ω_{01}	11.77	rad/s
ω_{02}	81.42	rad/s
f_{0a}	1.88	Hz
f_{0b}	12.94	Hz
ω_{0a}	11.78	rad/s
ω_{0b}	81.31	rad/s
c_{kr1}	3 769.9	N·s/m
c_{kr2}	5 691.8	N·s/m
c_{kra}	3 769.9	N·s/m
c_{krb}	5 691.8	N·s/m

4. Detailed description and evaluation of analysed variants of the 'theta' method

As it has been mentioned, the notion of a relative coefficient of damping [damping ratio] in the suspension system is used, which is denoted by the Greek letter ϑ ['theta'] – see equations [26]–[29]. Two versions of the method come from modal analysis and are also known as the 'peak-picking method' or 'half-power method' [9]. The other two versions are described in cited patent documentation [3, 11, 18].

4.1. The 'Calvo 1' and 'Calvo 2' methods

Both refer to the 'peak-picking method', also referred to as 'half-power method', known from modal analysis [9]. The quantities to be assessed may be the tire-exciter contact force F_{op} or the absolute value of transmittance H_{Fdz} of its dynamic component as well as of the corresponding measured values, i.e. F_{opm} and H_{Fmd} . The sense of selection of the values of the

quantities used in this method has been illustrated in Figure 5. In this case, a curve representing one of the quantities mentioned above is analysed in the area around its maximum.

In publication [4], the authors determined the value of the relative coefficient of damping in the suspension system ϑ_{C1} [the 'Calvo 1' coefficient] from equation [30]. The Hertz frequency f_{Cm} is here close to the 2nd resonance frequency. In publication [5], two modifications have been proposed: the use of a simpler form of the relative coefficient of damping in the suspension system ϑ_{C2} [the 'Calvo 2' coefficient – see equation [31]] and analysis for Hertz frequency f_{Cm} close to the 1st resonance frequency.

$$\vartheta_{C1} = \frac{f_{C2}^2 - f_{C1}^2}{4 \cdot f_{Cm}^2} \quad (30)$$

$$\vartheta_{C2} = \frac{f_{C2} - f_{C1}}{2 \cdot f_{Cm}} \approx \vartheta_{C1} \quad (31)$$

The approximation shown in relation [31] is acceptable when $f_{Cm} = (f_{C2} + f_{C1})/2$, i.e. when the curves under analysis are symmetric, which is not always true. As an example, this requirement is not met in the case illustrated in Figure 5. Therefore, a decision was made to analyse both variants of the Calvo method, and around both the 1st and 2nd resonance frequency at that.

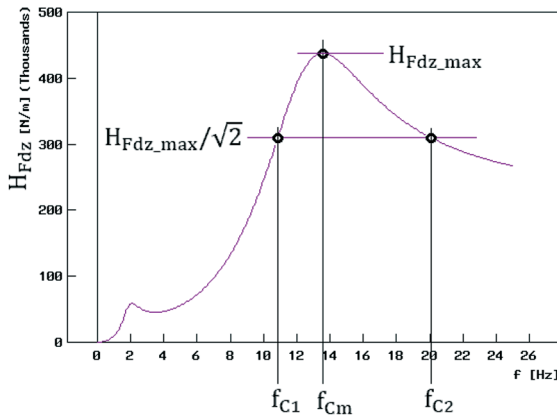


Fig. 5. The 'peak-picking' method, variants 'Calvo 1' and 'Calvo 2'. The absolute value of transmittance H_{Fdz} of force F_{dz} in the area around its maximum H_{Fdz_max} is analysed. f represents the Hertz frequency

Figures 6a and b and Figures 7a and b illustrate the applicability of the ‘Calvo 1’ and ‘Calvo 2’ methods to the analysis close to the 1st [Figures 6a and b] and 2nd [Figures 7a and b] resonance frequency, for the front suspension system of a medium-class motor car Astra Van. The absolute values of transmittances H_{Fdz} and H_{Fmd} of the tire-exciter contact force [Figures ‘a’] and of its measured value [Figures ‘b’] are analysed, respectively, in the areas around their maximums. Close to the 1st resonance frequency [Figures 6a and b], they are very similar to each other. The values of ϑ_{C1} , ϑ_{C2} , ϑ_{C1m} , and ϑ_{C2m} may be calculated for 6 of the 12 ϑ_I values under consideration. Close to the 2nd resonance frequency [Figures 7a and b], the ϑ_{C1} and ϑ_{C2} values may be calculated for 7 of the 12 ϑ_I values under consideration and the ϑ_{C1m} and ϑ_{C2m} values may be calculated for all the 12 ϑ_I values.

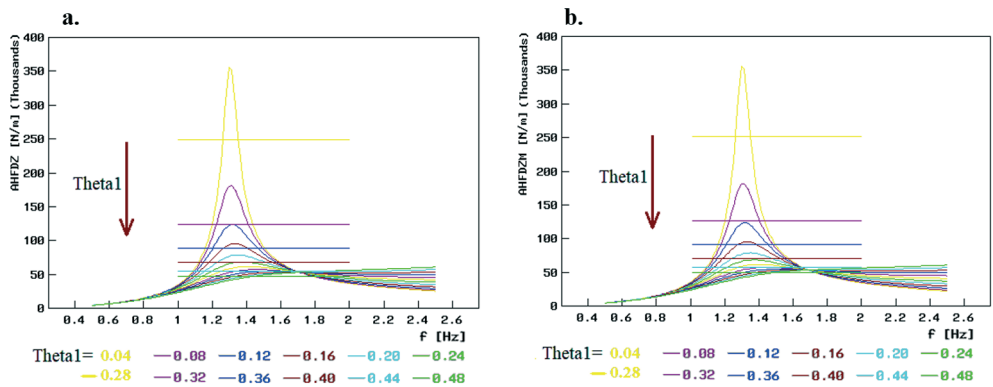


Fig. 6. Illustration of the applicability of the ‘Calvo 1’ and ‘Calvo 2’ methods to the analysis carried out close to the 1st resonance frequency. Analysed are the absolute values of transmittances H_{Fdz} [a] and H_{Fmd} [(b) - related to the tire-exciter contact force and to its measured value, respectively, and denoted by AHFDZ and AHFDZM in the graphs] close to their maximums.

Object tested: front suspension of the Astra Van

Figures 8a and b and Figures 9a and b show results obtained from methods ‘Calvo 1’ [ϑ_{C1} and ϑ_{C1m}] and ‘Calvo 2’ [ϑ_{C2} and ϑ_{C2m}] close to the 1st and 2nd resonance frequency of the front suspension system of a medium-class motor car Astra Van. Figures ‘a’ and ‘b’ deal with the absolute values of transmittances H_{Fdz} of the tire-exciter contact force and H_{Fmd} of the measured value of this force, respectively. For the 1st resonance frequency [Figures 8a and b], the values of ϑ_{C1} , ϑ_{C2} , ϑ_{C1m} , and ϑ_{C2m} well represent the value of ϑ_I , both in qualitative and quantitative terms, but only within the range of up to $\vartheta_I=0.24$. For the 2nd resonance frequency in turn [Figures 9a and b], the values of ϑ_{C1} , ϑ_{C2} , ϑ_{C1m} , and ϑ_{C2m} are close to the value of ϑ_I , but only if they are very low [not exceeding 0.16–0.20; within this range of ϑ_I , the errors are smaller for the ϑ_{C1m} and ϑ_{C2m} values measured].

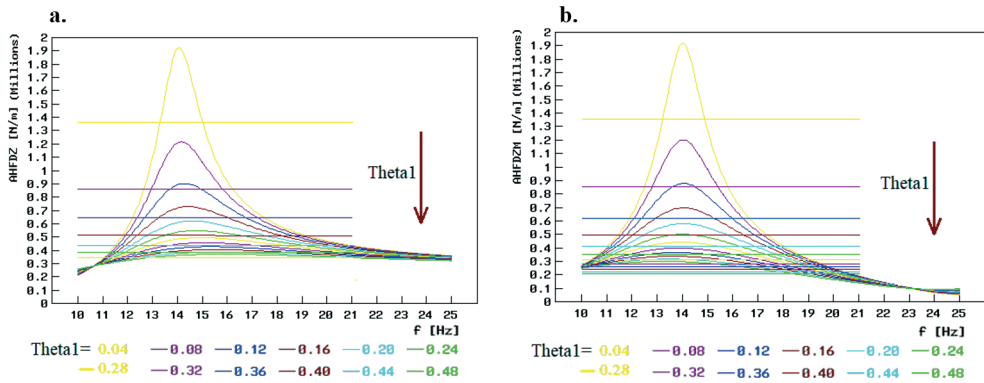


Fig. 7. Illustration of the applicability of the ‘Calvo 1’ and ‘Calvo 2’ methods to the analysis carried out close to the 2nd resonance frequency. Analysed are the absolute values of transmittances H_{FdZ} [a] and H_{Fmd} [(b) - related to the tire-exciter contact force and to its measured value, respectively, and denoted by AHFDZ and AHFDZM in the graphs] close to their maximums.
Object tested: front suspension of the Astra Van

It is hard to state unequivocally which of the ‘Calvo 1’ and ‘Calvo 2’ methods would offer better estimation of ϑ_I . This depends on the quantity analysed and on the ϑ_I value. A result markedly worse for the ‘Calvo 1’ method can be seen in Figure 9a for $\vartheta_I > 0.16$. The results obtained for the front suspension system of a medium-class motor car Astra Van indicate usefulness of the ‘Calvo 1’ and ‘Calvo 2’ methods for low ϑ_I values ($\vartheta_I < 0.16-0.20$), i.e. for shock absorbers being in medium and poor condition.

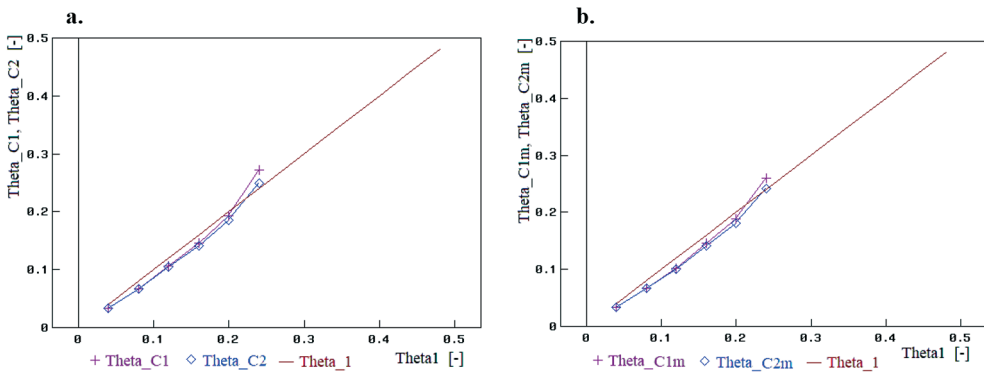


Fig. 8. Results obtained from methods ‘Calvo 1’ [ϑ_{C1} and ϑ_{C1m} , denoted by Theta_C1 and Theta_C1m in the graphs] and ‘Calvo 2’ [ϑ_{C2} and ϑ_{C2m} , denoted by Theta_C2 and Theta_C2m in the graphs] close to the 1st resonance frequency. Figures [a] and [b] deal with the absolute values of transmittances H_{FdZ} of the tire-exciter contact force and H_{Fmd} of the measured value of this force, respectively.
Object tested: front suspension of the Astra Van

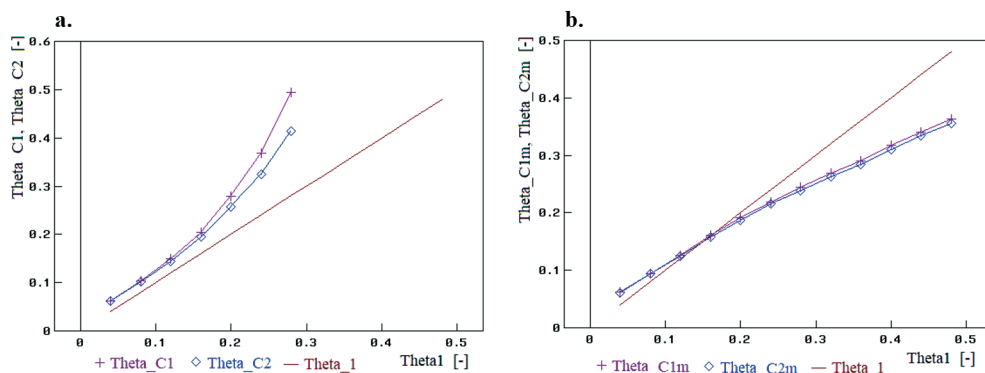


Fig. 9. Results obtained from methods ‘Calvo 1’ [ϑ_{C1} and ϑ_{C1m} , denoted by Theta_C1 and Theta_C1m in the graphs] and ‘Calvo 2’ [ϑ_{C2} and ϑ_{C2m} , denoted by Theta_C2 i Theta_C2m in the graphs] close to the 2nd resonance frequency. Figures (a) and (b) deal with the absolute values of transmittances H_{Fd_z} of the tire-exciter contact force and H_{Fmd} of the measured value of this force, respectively.
Object tested: front suspension of the Astra Van

Similar calculations were carried out for data of the rear suspension system of the same car. Close to the 1st resonance frequency, the values of ϑ_{C1} , ϑ_{C2} , ϑ_{C1m} , and ϑ_{C2m} could be calculated for 7 of the 12 ϑ_I values under consideration. Close to the 2nd resonance frequency, the ϑ_{C1} and ϑ_{C2} values could be calculated for 10 of the 12 ϑ_I values under consideration and the ϑ_{C1m} and ϑ_{C2m} values could be calculated for all the 12 ϑ_I values.

Figures 10a and b and Figures 11a and b show results obtained from methods ‘Calvo 1’ [ϑ_{C1} and ϑ_{C1m}] and ‘Calvo 2’ [ϑ_{C2} and ϑ_{C2m}] close to the 1st and 2nd resonance frequency. Figures ‘a’ and ‘b’ deal with the analysed absolute value of transmittance H_{Fd_z} of the tire-exciter contact force and the absolute value of transmittance H_{Fmd} of the measured value of this force, respectively.

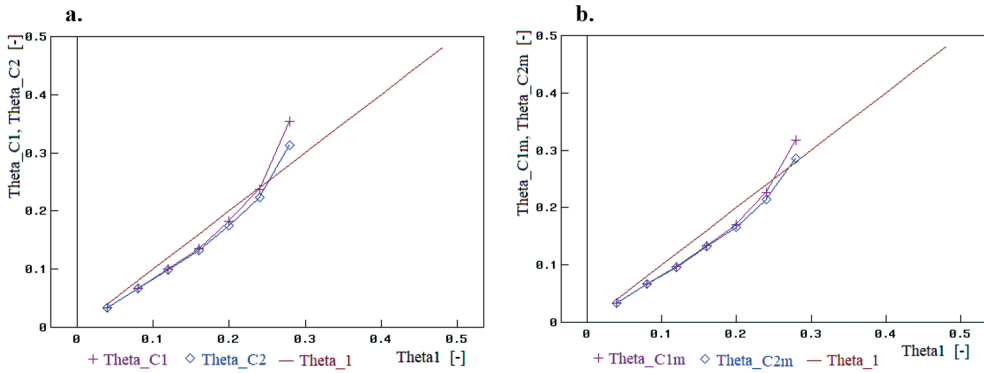


Fig. 10. Results obtained from methods 'Calvo 1' [ϑ_{C1} and ϑ_{C1m} , denoted by Theta_C1 and Theta_C1m in the graphs] and 'Calvo 2' [ϑ_{C2} and ϑ_{C2m} , denoted by Theta_C2 i Theta_C2m in the graphs] close to the 1st resonance frequency. Figures (a) and (b) deal with the analysed absolute value of transmittance H_{Fdc} of the tire-exciter contact force and the absolute value of transmittance H_{Fmd} of the measured value of this force, respectively. Object tested: rear suspension of the Astra Van

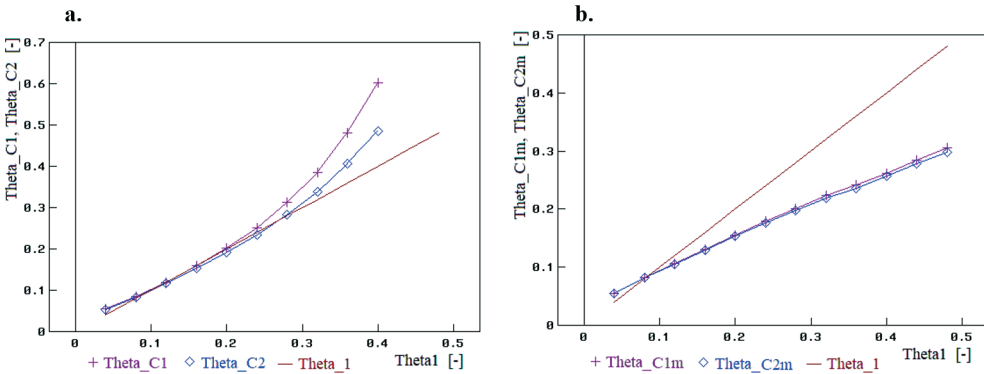


Fig. 11. Results obtained from methods 'Calvo 1' [ϑ_{C1} and ϑ_{C1m} , denoted by Theta_C1 and Theta_C1m in the graphs] and 'Calvo 2' [ϑ_{C2} and ϑ_{C2m} , denoted by Theta_C2 i Theta_C2m in the graphs] close to the 2nd resonance frequency. Figures (a) and (b) deal with the analysed absolute value of transmittance H_{Fdc} of the tire-exciter contact force and the absolute value of transmittance H_{Fmd} of the measured value of this force, respectively. Object tested: rear suspension of the Astra Van

For the 1st resonance frequency (Figures 10a and b), the values of ϑ_{C1} , ϑ_{C2} , ϑ_{C1m} and ϑ_{C2m} satisfactorily represent the value of ϑ_I , both in qualitative and quantitative terms, but only within the range of up to $\vartheta_I = 0.24$; however, these results are burdened with a greater error than it was in the case of the front suspension system. For the 2nd resonance frequency in turn (Figures 11a and b), the values of ϑ_{C1} and ϑ_{C2} are close to the value of ϑ_I within the range from 0.04 to 0.28. For the values exceeding 0.28, the results are overestimated, espe-

cially for the 'Calvo 1' method. The calculated ϑ_{C1m} and ϑ_{C2m} values are close to those of ϑ_I , but only for ϑ_I not exceeding 0.12. Above this level, the error rapidly increases with growing ϑ_I values, which are underestimated. It is hard to state unequivocally which of the 'Calvo 1' and 'Calvo 2' methods would offer better estimation of ϑ_I , except for the trend that can be seen in Figure 11a for the 'Calvo 1' method. The results obtained for the rear suspension system of a medium-class motor car Astra Van indicate usefulness of the 'Calvo 1' and 'Calvo 2' methods for the 1st resonance frequency unless the ϑ_I values exceed 0.24. For the 2nd resonance frequency, both methods are useful, but only for the analysis of the tire-exciter contact force, i.e. when the value measured is corrected by the force of inertia of exciter's vibration plate.

The presented results obtained for the front and rear suspension systems of a medium-class motor car Astra Van show that both the 'Calvo 1' and 'Calvo 2' methods are useful, but only for low and medium ϑ_I values (of up to $\vartheta_I=0.24$), i.e. for shock absorbers being in medium and poor condition. If the assessment is done for measurements carried out close to the 2nd resonance frequency, then the force value measured must be corrected by the force of inertia of exciter's vibration plate. In such a case, however, the assessment of the condition of the suspension system might be too optimistic [see Figure 9a]. The above assessment of the usefulness of the 'Calvo 1' and 'Calvo 2' methods may be confronted with nominal values of the relative damping coefficient ϑ_I for suspension systems of various kinds. The authors of publication [4] define the following grades of motor car suspension systems, based on the ϑ_I value: 0.20-0.25 – 'comfort'; 0.25-0.30 – 'semi-sport'; 0.30-0.35 – 'sport'; 0.35-0.40 – 'racing'.

4.2. The Mazůrek and Klapka method

A description of this method may be found in the patent application submitted by Ivan Mazůrek and Milan Klapka [18] and in the publication by these authors [11]. In relation to the Hunter method [e.g. [20, 22, 23]], the authors propose to use the stand with a smaller mass forcing vibrations and a smaller amplitude of its vertical movement. The essence of the method does not change: the phase shift angle between the kinematic excitation (plate movement) and the force in contact of the tire with the excitation plate is tested. The relative suspension damping coefficient ϑ_{Cz} being determined is described by equation [32]. Formally, it is related to the quantity ϑ_b defined by [29], but it is a theoretical notion applicable to the model of Figure 4b instead of being related to the quantity to be found, which should reflect the ϑ_I values applicable to Figures 3a and b. The equation has been derived from the relations that define the phase shift angle between the vertical displacement of exciter's vibration plate and the tire-exciter contact force for the resonance frequency, calculated on the grounds of transmittance $H_{Fdz}(i\omega)$.

$$\vartheta_{Cz} = \frac{k_2}{2 \cdot (k_1 + k_2) \cdot t g \phi(\omega_{0b})} \approx \frac{1}{2 \cdot t g \phi(\omega_{0b})} \quad (32)$$

Φ is the said phase shift angle; k_1 , k_2 and $\omega_{0b} = 2 \cdot \pi \cdot f_{0b}$ are parameters of the system of Figure 4b; ω_{0b} and f_{0b} are defined by equations [20] and [21], respectively. The approximate form on the right side of equation [32] is acceptable for $k_2 \gg k_1$. Equation [20] suggests that ω_{0b} is

close to the 2nd natural frequency of the ‘quarter-car’ model of Figure 3a (this is confirmed by the values of the parameters of the models under test), for which the relation $m_1 \gg m_2$ is true and the high value of frequency ω_{0b} justifies the assumption that $z_I=0$. Thus, the system of Figure 3a comes down to the system of Figure 4b. The authors of publications [11, 18] do not make any mention of considering the inertia of the vibration plate. The author of this study decided to examine the impact of this inertia on the results obtained with using this method. The relative damping coefficient calculated from the phase shift angle determined without considering the inertia of the vibration plate, i.e. based on the force measured in the tester, was denoted by ϑ_{Czm} . The sensitivity of coefficient ϑ_{Cz} [equation (32)] to changes in the frequency at which the measurement is carried out was also examined. The relative sensitivity coefficient $W_{Cz}^{\%}$ [equation (33)] was determined; it is measured in %/%, which means that it represents the relative percentage change in ϑ_{Cz} caused by a one percent change in the excitation frequency ω .

$$W_{Cz}^{\%} = \frac{\partial(\ln \vartheta_{Cz})}{\partial(\ln \omega)} = \frac{\partial(\vartheta_{Cz})}{\partial(\omega)} \cdot \frac{\omega}{\vartheta_{Cz}} = -\frac{1 + (tg\phi(\omega))^2}{tg\phi(\omega)} \cdot \frac{\partial\phi}{\partial\omega} \cdot \omega \quad \text{for } \omega = \omega_{0b} \quad (33)$$

Figure 12a and b shows the effect of using the method under consideration for data of the front [Figure a) and rear [Figure b) suspension system of a medium-class motor car Astra Van. The ϑ_{Cz} and ϑ_{Czm} coefficients have been calculated for the phase shift angle and for $\omega_{0b} = 2 \cdot \pi \cdot f_{0b}$ of the simplified undamped system.

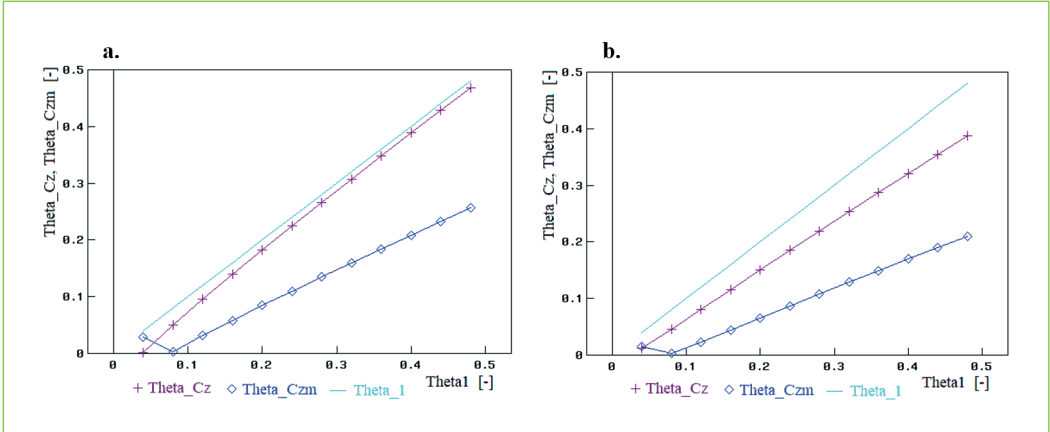


Fig. 12. Results obtained with using the Mazúrek and Klapka method for data of the front [a) and rear [b) suspension of the Astra Van. The ϑ_{Cz} and ϑ_{Czm} coefficient values [Theta_Cz and Theta_Czm, respectively, in the graphs] have been calculated for the phase shift angle and for $\omega_{0b} = 2 \times \pi \times f_{0b}$ of the simplified undamped system. The ϑ_{Cz} values apply to the measurement of the phase shift of the tire-exciter contact force and the ϑ_{Czm} values apply to the measurement of the phase shift of the force measured in the tester [where the impact of the force of inertia of exciter's vibration plate is not considered]

The ϑ_{Cz} values apply to the measurement of the phase shift of the tire-exciter contact force and the ϑ_{Czm} values apply to the measurement of the phase shift of the force measured in

the tester (where the impact of the force of inertia of exciter's vibration plate is not considered). Both graphs confirm the reasonability of considering the inertia of exciter's vibration plate. When the related correction is made, the results calculated for the front suspension system become close to the actual values ($\vartheta_{Cz} \approx \vartheta_I$). For the rear suspension system, the results are not so satisfactory; nevertheless, the $\vartheta_{Cz}(\vartheta_I)$ curve is almost parallel to the $\vartheta_I = \vartheta_I$ line.

Figures 13a and b show results of estimation of the relative sensitivity coefficient $W^{%}_{Cz}$, which represents the relative percentage change in ϑ_{Cz} caused by a one percent change in the excitation frequency ω . The $W^{%}_{Cz}$ coefficient values apply to the measurement of the phase shift of the tire-exciter contact force and the $W^{%}_{Czm}$ values apply to the measurement of the phase shift of the force measured in the tester (where the impact of the force of inertia of exciter's vibration plate is not considered). These calculations were carried out for $\omega_{0b} = 2 \cdot \pi \cdot f_{0b}$, corresponding to the natural frequency of the simplified undamped system shown in Figure 4b.

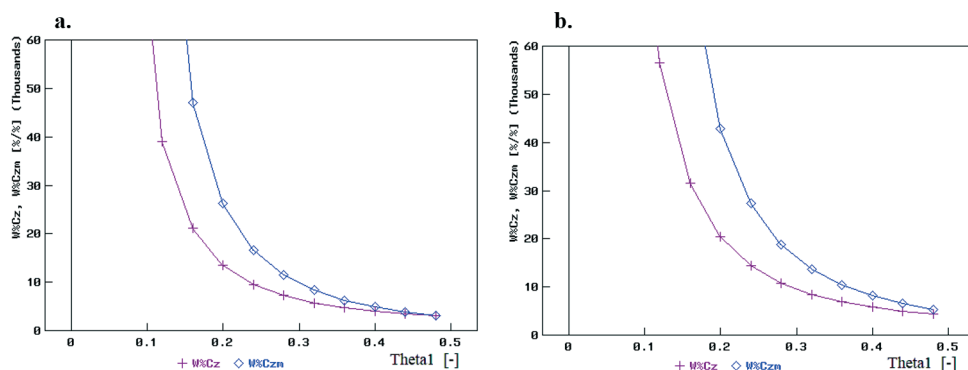


Fig. 13. Results obtained with using the Mazúrek and Klapka method for data of the front [a] and rear [b] suspension of the Astra Van. The relative sensitivity coefficient $W^{%}_{Cz}$ represents the relative percentage change in ϑ_{Cz} caused by a one percent change in the excitation frequency ω . The $W^{%}_{Cz}$ coefficient values apply to the measurement of the phase shift of the tire-exciter contact force and the $W^{%}_{Czm}$ values apply to the measurement of the phase shift of the force measured in the tester (where the impact of the force of inertia of exciter's vibration plate is not considered)

The results indicate very high sensitivity of the method under analysis to the accuracy of determining the frequency for which the phase shift angle is measured and the ϑ_{Cz} value is calculated. This sensitivity rises with a decrease in damping, i.e. with growing deterioration in the condition of vibration damping elements of the suspension system.

The results presented indicate considerable disadvantages of the Mazúrek and Klapka method. It has been clearly shown that a correction must be made here for the inertia of exciter's vibration plate. This is because the measurement is carried out at the higher reso-

nance frequency of the undamped system. Moreover, the method under analysis has been shown to be very sensitive to the accuracy of determining the frequency at which the measurement is carried out. This sensitivity rises with a decrease in damping, i.e. with growing deterioration in the condition of vibration damping elements of the suspension system. This must be considered a serious drawback of the method in question.

4.3. The Buzzi method

This method has been described in the patent application submitted by Carlo Buzzi [3]. The hardware of the method is like this used in the Hunter method [e.g. [20, 22, 23]]. Measuring system is focused on the phase shift angle between the excitation (plate movement) and the force in the tire–excitation plate contact. The software is created to measure of phase shift angle derivative related to excitation frequency. The relative suspension damping coefficient ϑ_{IT} being determined is described by equation [34]. Formally, it is related to the quantity ϑ_a defined by [28], but it is a theoretical notion applicable to the model of Figure 4a instead of being related to the quantity to be found, which should reflect the ϑ_I values applicable to Figures 3a and b. Φ is the phase shift angle between the tire–exciter contact force and the vertical displacement of exciter's vibration plate; $\omega=2\cdot\pi\cdot f$ [f is the Hertz frequency] and $\omega_{0a}=2\cdot\pi\cdot f_{0a}$ is a parameter of the system of Figure 4a; ω_{0a} and f_{0a} are defined by equations [19] and [21], respectively.

$$\vartheta_{IT} = \frac{1}{\frac{\partial\Phi}{\partial\omega}\omega_{0a}} \quad (34)$$

The method has been derived from an analysis of the derivative of Φ with respect to ω . The analysis applies to a 1DOF system shown in Figure 4a and built by simplifying the system of Figure 3a. The unsprung mass m_2 is disregarded (although in practice, however, it is most convenient to assume $m=m_1+m_2$). The suspension stiffness k is the resultant stiffness of a series system of springs with stiffness of k_1 and k_2 . If this is considered, it becomes clear that equation [19] suggests the value of ω_{0a} to be close to that of the first natural frequency ω_{0I} of the model shown in Figure 4a (which is confirmed by the values of the parameters of the models under examination). In the Carlo Buzzi's patent specification [3], no mention has been made of considering the inertia of tester's vibration plate. This may be understood if considering the low value of the frequency for which equation [34] is used. The author of this study, however, decided to examine the impact of this inertia on the results obtained with using this method. The relative damping coefficient calculated from the phase shift angle determined without considering the inertia of the vibration plate, i.e. based on the value of the force measured in the tester, was denoted by ϑ_{ITzm} . The sensitivity of coefficient ϑ_{IT} [equation [34]] to changes in the frequency at which the measurement is carried out was also examined. The relative sensitivity coefficient $W_{IT}^{\%}$ [equation [35]] was determined; it is measured in %/%, which means that it represents the relative percentage change in ϑ_{IT} caused by a one percent change in the excitation frequency ω .

$$W_{IT}^{\%} = \frac{\partial(\ln\vartheta_{IT})}{\partial(\ln\omega)} = \frac{\partial(\vartheta_{IT})}{\partial(\omega)} \cdot \frac{\omega}{\vartheta_{IT}} = -\frac{\frac{\partial^2\Phi}{\partial\omega^2}\omega + \frac{\partial\Phi}{\partial\omega}}{\frac{\partial\Phi}{\partial\omega}} \quad \text{for } \omega=\omega_a \quad (35)$$

For the $\Phi(\omega)$ curves, representing the phase shift angle as a function of the excitation frequency, approximations of derivatives of angle Φ with respect to frequency ω were determined [with using a difference quotient] to enable the calculation of ϑ_{IT} and ϑ_{ITm} for frequency ω_{0a} . Figure 14 a and b shows the effect of using the Buzzi method for data of the front [Figure a] and rear [Figure b] suspension system of a medium-class motor car Astra Van. The ϑ_{IT} and ϑ_{ITm} coefficients have been calculated for the phase shift angle and for natural frequency $\omega_{0a}=2\pi f_{0a}$ of the simplified undamped system. The ϑ_{IT} values apply to the measurement of the phase shift of the tire-exciter contact force and the ϑ_{ITm} values apply to the measurement of the phase shift $\Phi_m(f)$ of the force measured in the tester [where the impact of the force of inertia of exciter's vibration plate is not considered]. Both graphs confirm the conjecture that the considering of the inertia of exciter's vibration plate is a matter of minor importance. For both the front and rear suspension system, the results obtained are very close to the actual values [i.e. ϑ_{IT} and ϑ_{ITm} are close to ϑ_I]. Over the ϑ_I range from zero to about 0.32 [very important from the point of view of diagnostics of motor car suspension system], errors are small, although greater for the rear suspension. Attention should be paid to the fact that for the system without suspension damping and for $\omega=\omega_{0a}$ ($f=f_{0a}$), the absolute value of the derivative of angle Φ with respect to frequency ω approaches infinity, i.e. ϑ_{IT} and ϑ_{ITm} approach zero, which shows that equation [34] is true. For the system with non-zero suspension damping and for $\omega=\omega_{0a}$, the absolute value of the derivative of angle Φ with respect to frequency ω is higher than zero. This derivative is the smaller the greater the damping in the suspension. This results in growing ϑ_{IT} and ϑ_{ITm} values, in accordance with equation [34].

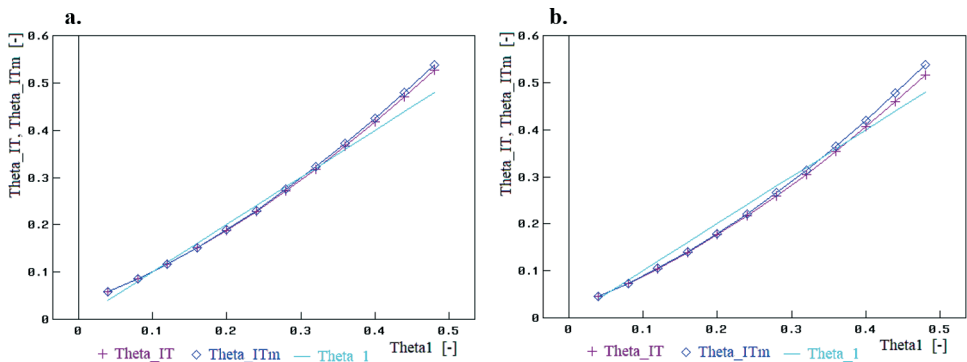
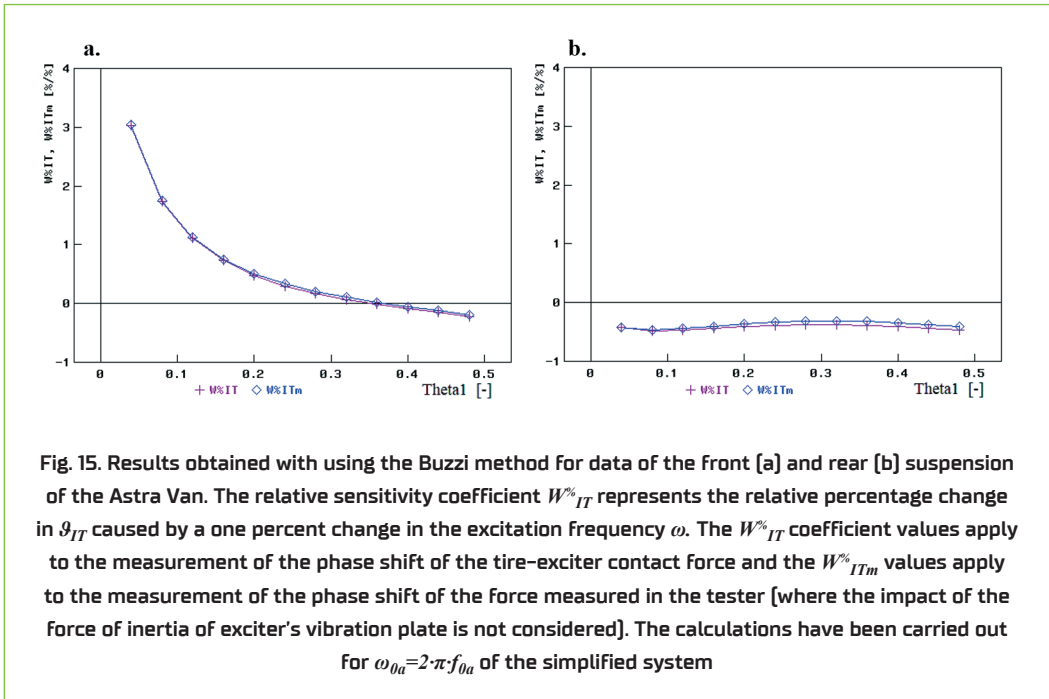


Fig. 14. Results obtained with using the Buzzi method for data of the front (a) and rear (b) suspension of the Astra Van. The ϑ_{IT} and ϑ_{ITm} coefficient values [Theta_IT and Theta_ITm, respectively, in the graphs] have been calculated for the phase shift angle and for $\omega_{0a}=2\pi f_{0a}$ of the simplified system. The ϑ_{IT} values apply to the measurement of the phase shift of the tire-exciter contact force and the ϑ_{ITm} values apply to the measurement of the phase shift of the force measured in the tester [where the impact of the force of inertia of exciter's vibration plate is not considered]

Figures 15a and b show results of estimation of the relative sensitivity coefficient $W_{IT}^{\%}$, which represents the relative percentage change in ϑ_{IT} caused by a one percent change in the excitation frequency ω . The $W_{IT}^{\%}$ coefficient values apply to the measurement of the phase shift of the tire-exciter contact force and the $W_{ITm}^{\%}$ values apply to the measurement of the phase shift of the force measured in the tester [where the impact of the force of inertia of exciter's vibration plate is not considered]. These calculations were carried out for $\omega_{0a}=2\cdot\pi\cdot f_{0a}$, corresponding to the natural frequency of the simplified undamped system shown in Figure 4a. The results indicate very low sensitivity of the method under analysis to the accuracy of determining the frequency for which the phase shift angle is measured and the ϑ_{IT} value is calculated. This sensitivity slightly rises [but for the front suspension system only] with a decrease in damping, i.e. with growing deterioration in the condition of vibration damping elements of the suspension system. Nevertheless, the sensitivity values still do not exceed 3 %/%, which is a very good point of this method. The results presented also indicate other considerable advantages of the Buzzi method [3]. It has been shown that any corrections to compensate the inertia of exciter's vibration plate are of no importance in this method.

The calculation results also show that this method is almost insensitive to the accuracy of determining the frequency at which the measurement is carried out. However, this low sensitivity may cause difficulties with measurements of the phase shift angle and its first and second derivative with respect to the excitation frequency.



5. Conclusions

The linear ‘quarter-car’ models used, and the frequency domain analysis provide grounds for general qualitative and (within a limited scope) quantitative assessment of usefulness of individual methods of evaluation of damping in suspension systems. In the two-degrees-of-freedom (2DOF) model used in the work, the impact of vibration plate’s mass on test results is considered. In some methods, such a model is simplified to a one-degree-of-freedom (1DOF) model. Not always the simplification of this kind is reasonable. Designers of diagnostic suspension testers introduce corrections to the measurement results in order to compensate the impact of weight of exciter’s vibration plate (by zeroing tester’s measuring systems before placing a vehicle on the tester). However, only very few of them consider a correction related to the inertia of the plate. Detailed conclusions concerning individual variants of the ‘theta’ method, analysed in this work, have been presented below. Table 3 presents a summary of the main remarks.

The ‘Calvo 1’ and ‘Calvo 2’ variants. Both produce similar results. Differences become apparent in the case of significant asymmetry in the curves characterizing the system under test, which not always takes place. These variants may be used to analyse the response of the system under test close to the 1st and 2nd resonance frequency. For the lower frequency, however, difficulties in the measurements may be encountered, related to the less distinct form of the maximum in the system response curve. The results presented here and obtained for the front and rear suspension systems of a medium-class motor car show that both of these variants are useful, but only for low and medium ϑ_I values (of up to $\vartheta_I=0.24$), i.e. for shock absorbers being in medium and poor condition. If the assessment is based on measurements carried out close to the 2nd (higher) resonance frequency, then the force value measured must be corrected by the force of inertia of exciter’s vibration plate. In such a case, however, the assessment of the condition of the suspension system might be too optimistic.

The variant proposed by Ivan Mazůrek and Milan Klapka. The results presented indicate considerable disadvantages of this variant. It has been shown that a correction must be made here for the inertia of exciter’s vibration plate, because the measurement is carried out at the higher resonance frequency. This variant is very sensitive to the accuracy of determining the frequency at which the measurement is carried out. The said sensitivity rises with a decrease in damping, i.e. with growing deterioration in the condition of vibration damping elements of the suspension system. This must be considered a serious drawback of the variant in question.

The variant proposed by Carlo Buzzi. This variant has important good points. Any corrections to compensate the inertia of exciter’s vibration plate are of no importance. The calculation results also show that in this case, the assessment of the condition of damping elements in the suspension system is almost insensitive to the accuracy of determining the frequency at which the measurement is carried out and to the accuracy of calculation of the relative damping in the suspension system. A weak point of this variant is the fact that the measurements are carried out here at a low frequency, which may cause difficulties with measurements of the phase shift angle and its first and second derivative with respect to the excitation frequency.

Table 3. Summary of the main remarks

The method	Main advantages	Main drawbacks	Recommendations for use	Necessary adjustments
Calvo 1	Insensitive to the asymmetry of the analyzed characteristics.	Measurement difficulties for the 1 st resonance frequency.	2 nd resonant frequency of the tested system. Lower range of relative damping (down to about 0.24).	Need to apply a correction resulting from the inertia of the vibration-inducing plate (for 2 nd resonance frequency). For the indicated 2 nd resonance frequency, it is too optimistic or too pessimistic for higher damping.
Calvo 2		Sensitive to the asymmetry of the analyzed characteristics. Measurement difficulties for the 1 st resonance frequency.	As above	As above
Mazúrek and Klapka		High sensitivity to the accuracy of determining the resonance frequency.	2 nd resonant frequency of the tested system.	Need to apply a correction resulting from the inertia of the vibration-inducing plate.
Buzzi	No need to apply a correction resulting from the inertia of the vibration-inducing plate. Low sensitivity to the accuracy of determining the resonance frequency.	Low frequency tests are associated with measurement difficulties.	1 st resonant frequency of the tested system.	

For practical application, the author suggests using a combination of at least two considered methods. It is possible because described methods use similar hardware structure components.

6. Closing remarks and future work

For all the variants of the 'theta' method, their correctness should be verified during calculations using non-linear models. Nonlinearities may change the behavior of the system and may be an interesting reason for specific isolating properties. It is important to put attention to dry friction in the suspension system, asymmetry of shock absorber damping curves, 'bouncing', i.e. tire separation from the exciter as well as nonlinearities of suspension and tire elasticity characteristics. The impact of transient states arising from changes in the excitation frequency during the diagnostic test should be evaluated. The results obtained must also be verified experimentally for the correctness and usefulness of the simulation test results to be assessed.

7. Acknowledgement

The work was done within project "UNILINE QUANTUM [...]" partially sponsored by the European Union within the European Regional Development Fund, Smart Growth Operational Programme, Sub-measure 1.1.1. Project No: POIR.01.01.01-00-0949/15 as well as by UNIMETAL Sp. z o.o. in Złotów.

8. References

- [1] Arczyński St.: *Mechanika ruchu samochodu* [Mechanics of motion of a motor vehicle], WNT, Warszawa, 1993.
- [2] Buekenhoudt P. (GOCA): Minimum phase shift. CITA 2011 Conference and 15th General Assembly, 2011, 4-6 May, Berlin, Germany.
- [3] Buzzi C. [inventor]: System for measuring the damping coefficient of vehicle-mounted shock absorbers. Appl. No EPO647843A2. European Patent Office: 12.04.1995. Bulletin 95/15.
- [4] Calvo J.A., Díaz V., San Román J.L.: Establishing inspection criteria to verify the dynamic behaviour of the vehicle suspension system by a platform vibrating test bench. *International Journal of Vehicle Design*. 2005, 38(4), 290-306, DOI: 10.1504/IJVD.2005.007623.
- [5] Calvo J.A., San Román J.L., Alvarez-Caldas C.: Procedure to verify the suspension system on periodical motor vehicle inspection. *International Journal of Vehicle Design*. 2013, 63(1), 1-17, DOI: 10.1504/IJVD.2013.055497.
- [6] Dixon J.C.: *The shock absorber handbook*, 2nd edition, SAE International, John Wiley & Sons Ltd. ISBN 978-0-7680-1843-1. November 2007.
- [7] Dukkupati R.V., Pang J., Qatu M.S., Sheng G., Shuguang Z.: *Road vehicle dynamics*. SAE International, Warrendale, Pa, 2008, ISBN 978-0-7680-1643-7.
- [8] Gardulski J.: Metody badań amortyzatorów samochodów osobowych [Testing methods for vehicle shock absorbers]. *Diagnostyka*. 2009, 3(51), 93-100.
- [9] He J., Fu Z.: *Modal analysis*. Butterworth-Heinemann, 2001, DOI: 10.1016/B978-0-7506-5079-3.X5000-1.
- [10] Kamiński E., Pokorski J.: *Teoria samochodu. Dynamika zawiesznień i układów napędowych pojazdów samochodowych* [Automobile theory. Dynamics of suspension systems and powertrains of motor vehicles]. WKŁ, Warszawa, 1983.

-
- [11] Klapka M., Mazůrek I., Macháček O., Kubik M.: Twilight of the EUSAMA diagnostic methodology. *Meccanica*, 2016, 52(9), 2023–2034, DOI: 10.1007/s11012-016-0566-0.
- [12] Klapka M., Mazůrek I., Kubik M., Macháček O.: Reinvention of the EUSAMA diagnostic methodology. *International Journal of Vehicle Design*. 2017, 74(4), 304–318, DOI: 10.1504/IJVD.2017.087968.
- [13] Knestel A., Küchle J. (inventors): Procedure and device for determining a measure of the vibration absorption of vehicles, European Patent EP1564538B1, European Patent Office, Bulletin 2010/23. Current Assignee: MAHA GmbH&Co.
- [14] Konieczny Ł.: Wykorzystanie metod drganiowych w ocenie stanu technicznego mechanicznych i hydropneumatycznych zawieszzeń pojazdów samochodowych [Application of vibratory methods for assessment of technical condition of mechanical and hydropneumatic automotive suspension systems], Wydawnictwo Politechniki Śląskiej, Gliwice, 2015.
- [15] Lozia Z.: The use of a linear quarter-car model to optimize the damping in a passive automotive suspension system – a follow-on from many authors' works of the recent 40 years, *The Archives of Automotive Engineering – Archiwum Motoryzacji*. 2016, 71(1), 33–65, DOI: 10.14669/AM.VOL71.ART3.
- [16] Lozia Z., Pirsztuk J.: Ocena wpływu sprzężeń w zawieszeniu samochodu na wyniki testu stanu amortyzatorów metodą EUSAMA [Assessment of the impact of couplings in the motor vehicle suspension system on EUSAMA shock absorber test results], Teka Komisji Naukowo-Problemovej Motoryzacji, PAN Oddział w Krakowie [Files of the Scientific and Problem Committee of the Automotive Industry, Polish Academy of Sciences, Division in Cracow, Kraków, 2001, 22, 273–280.
- [17] Lozia Z., Zdanowicz P.: Simulation assessment of the impact of inertia of the vibration plate of a diagnostic suspension tester on results of the EUSAMA test of shock absorbers mounted in a vehicle. *IOP Conference Series: Materials Science and Engineering*. 2018, 421(2), 022018, DOI: 10.1088/1757-899X/421/2/022018.
- [18] Mazůrek I., Klapka M. (inventors): Method of measuring damping ratio of unsprung mass of half axles of passenger cars using a suspension testing rig without disassembling, Appl. No. EP3193152A1, European Patent Office: 19.07.2017. Bulletin 2017/29.
- [19] Pérez-Peña A., García-Granada A.A., Menacho J., Molins J.J., Reyes G.: A methodology for damping measurement of engineering materials: Application to a structure under bending and torsion loading. *Journal of Vibration and Control*. 2016, 22(10), 2471–2481, DOI: 10.1177/1077546314547728.
- [20] Stańczyk T. L.: Analysis of the possibilities of using the phase angle as a diagnostic parameter in shock absorber examinations. *Archives of Transport*. 2004, 16(2), 33–50.
- [21] Stańczyk T. L., Jurecki R.: Analiza porównawcza metod badania amortyzatorów hydraulicznych [Comparative analysis of testing methods of hydraulic shock absorbers]. *Proceedings of the Institute of Vehicles, Warsaw University of Technology*, 2014, 4(100), 25–45.
- [22] Tsymberov A. (inventor): Suspension tester and method, United States Patent No. 5,369,974. Date of Patent: Dec. 6, 1994.
- [23] Tsymberov A.: An improved non-intrusive automotive suspension testing apparatus with means to determine the condition of the dampers. *SAE Technical Paper*. 1996, 105, 970–983, DOI: 10.4271/960735.
- [24] Wang X., Kun L., Liu H., He Y.: Damping identification with acceleration measurements based on sensitivity enhancement method. *Shock and Vibration*. 2018, 1, 1–16, DOI: 10.1155/2018/6476783.
- [25] Zdanowicz P.: Ocena stanu amortyzatorów pojazdu z uwzględnieniem tarcia suchego w zawieszeniu [Assessment of the condition of vehicle's shock absorbers with considering the dry friction in the suspension system], doctoral dissertation, Warsaw University of Technology, Faculty of Transport, Warszawa, 2012.